Robust Cubature Kalman Filter for Dynamic State Estimation of Synchronous Machines Under Unknown Measurement Noise Statistics

YANG LI[ID][1]**, (Senior Member, IEEE), JING LI**[1]**, JUNJIAN QI**[ID][2]**, (Senior Member, IEEE), AND LIANG CHEN**[3]

[1]School of Electrical Engineering, Northeast Electric Power University, Jilin 132012, China
[2]Department of Electrical and Computer Engineering, University of Central Florida, Orlando, FL 32816, USA
[3]State Grid Heibei Economic Research Institute, Shijiazhuang 050041, China

Corresponding author: Yang Li (liyang@neepu.edu.cn)

ABSTRACT The Kalman-type filtering techniques including cubature Kalman filter (CKF) does not work well in non-Gaussian environments, especially in the presence of outliers. To solve this problem, Huber's M-estimation-based robust CKF (RCKF) is proposed for synchronous machines by combining the Huber's M-estimation theory with the classical CKF, which is capable of coping with the deterioration in performance and discretization of tracking curves when measurement noise statistics deviate from the prior noise statistics. The proposed RCKF algorithm has good adaptability to unknown measurement noise statistics characteristics including non-Gaussian measurement noise and outliers. The simulation results on the WSCC 3-machine 9-bus system and New England 16-machine 68-bus system verify the effectiveness of the proposed method and its advantage over the classical CKF.

INDEX TERMS Dynamic state estimation, cubature Kalman filter, synchronous machines, M-estimation theory, unknown noise statistics, non-Gaussian noise, outliers, PMU data.

I. INTRODUCTION
A. MOTIVATION

Accurate and reliable dynamic state information of synchronous machines plays a crucial role in real-time monitoring, protection, and control of power systems [1], [2]. In addition, the emerging application of situational awareness puts forward higher requirements for the status information acquisition as the system states evolve more complexly and quickly due to increasing cyber attacks [3] and high penetrations of renewable generations [4], [5]. However, some important synchronous machine state variables cannot be directly obtained. The successful industrial application of wide-area measurement system has recently made possible the estimation of all the state variables of a synchronous machine through the use of dynamic state estimations (DSE) [6]. Meanwhile, there is a higher-level requirement on DSE to ensure the safe and economic operation of a modern power system since its operation is increasingly close

to the limits due to growing electricity demands and limited investments. Therefore, it is a pressing and challenging task to develop an effective DSE approach for synchronous generators.

B. LITERATURE REVIEW

The term ''dynamic state estimation'' was first used in the 1970s [7], in which a Kalman filter technique was utilized to improve the performance of conventional quasi-static state estimation for power systems. In recent years, the studies on state estimators began to focus on a synchronous generator and its electromechanical transient model [8]–[10]. In essence, this is a typical nonlinear filter problem. Up to now, there has been a significantly amount of studies on DSE of synchronous machines by using particle filters (PF) [11], [12] and various Kalman-type filtering algorithms, such as extended Kalman filter (EKF) [13]–[17], unscented Kalman filter (UKF) [18]–[24], and Cubature Kalman Filter (CKF) [3], [25], [26]. The EKF is a classical nonlinear Kalman filter; the unscented transform-based UKF provides reasonable filtering performance, but its

---

The associate editor coordinating the review of this manuscript and approving it for publication was Lin Zhang.

convergence is dependent on the sampling methods of Sigma points [18], [19]; the CKF based on the spherical-radial cubature rule is an emerging nonlinear filter, which can give a systematic solution for high-dimensional nonlinear filtering issues. Extensive comparisons of all these Kalman-type estimators have been made from different perspectives, such as convergence, numerical stability, and computational complexity in [3] and [16].

C. LIMITATIONS AND CONTRIBUTIONS

The Kalman-type filtering techniques perform well under the Gaussian assumption [3], [5], [27]. However, the distribution of the measurement noise may not obey this assumption in practical applications. Recent research findings in [28] demonstrate that the errors in PMU measurements such as voltage phasors tend to follow non-Gaussian distributions with long tails such as Laplace distribution and often contain high-intensity noise realizations, called outliers, which could deteriorate the performance of the Kalman-type filtering approaches. Furthermore, the received measurements may be biased because of multiple reasons such as false data injection (FDI) attacks [3], [29]. Therefore, there is sustainable motivation for developing a robust filter that can work well in non-Gaussian environments and in the presence of outliers. In order to achieve such a goal, the work in [30] proposes a Generalized-Maximum Likelihood (GM)-UKF, in which a batch-mode regressing form is obtained via the statistical linearization to enhance the data redundancy, and thereby the form enables the GM-estimator to identify bad data and filter out unknown noises. However, when using the UKF, it is an essential but challenging task to generate Sigma points by using a scaled symmetric sampling strategy in case the state vector dimension is greater than 3, since there are three mutually influential parameters needed to be tuned in this step, while there is currently no consensus about the corresponding parameter selection principles.

In this work, a robust CKF (RCKF) based distributed DSE approach is developed to estimate the machine dynamic states by integrating the Huber's M-estimation theory with the CKF. Different from the GM-type estimator in [30], the proposed RCKF uses the robust M-estimation to detect outliers in measurements and then eliminates them by revising measurement noise variance matrix.

The main contributions of this work are as follows.

(1) A novel DSE algorithm, called RCKF, is proposed for synchronous machines by combining the Huber's M-estimation theory with the classical CKF, which has the ability to cope with the deterioration in performance and discretization of tracking curves when measurement noise statistics deviate from the prior noise statistics.

(2) The simulation results on the WSCC 3-machine 9-bus system and New England 16-machine 68-bus system demonstrate that the proposed approach is capable of addressing the DSE of synchronous machines under unknown measurement noise statistics.

(3) By sacrificing computational efficiency slightly, the proposed algorithm outperforms the conventional CKF under all the used noise conditions, including non-Gaussian measurement noise and outliers.

D. PAPER ORGANIZATION

The remainder of this paper is structured as follows. The used estimation models are introduced in Section II. Section III presents the proposed RCKF in detail. Section IV gives case studies to examine the proposed approach. And finally, the conclusions are drawn in Section V.

II. ESTIMATION MODELS

A. SYNCHRONOUS MACHINE MODEL

Fourth-order transient model is a well-known generator model that has been extensively studied in previous literature [1], [9], [10], [21]. Its mathematical model is

$$\begin{cases} \dot{\delta} = \omega_0 \Delta\omega \\ \Delta\dot{\omega} = \dfrac{1}{T_J}\left[T_m - T_e - D\Delta\omega\right] \\ \dot{E}_q' = \dfrac{1}{T_{d0}'}\left[E_f - E_q' - \left(X_d - X_d'\right)I_d\right] \\ \dot{E}_d' = \dfrac{1}{T_{q0}'}\left[-E_d' + \left(X_q - X_q'\right)I_q\right] \end{cases} \quad (1)$$

$$\begin{cases} I_d = \dfrac{E_q' - U_t\cos(\delta - \phi)}{X_d'} \\ I_q = \dfrac{U_t\sin(\delta - \phi) - E_d'}{X_q'} \end{cases} \quad (2)$$

where δ and ω are respectively the rotor angle and speed; E_q' and E_d' are the q-axis and d-axis transient voltages; T_m is the mechanical torque; T_e is the electromagnetic torque; D is damping coefficient; T_{d0}' and T_{q0}' are respectively the d- and q- axes transient time constants; E_f is the field voltage; X_q and X_q' are q-axis synchronous and transient reactance; X_d and X_d' are the d-axis synchronous and transient reactance; U_t and ϕ are the magnitude and phase angle of the generator terminal voltage, respectively; I_d and I_q are the d-axis and q-axis generator output currents.

The measurement equations are given by

$$\begin{cases} \omega^z = \omega \\ \delta^z = \delta \\ P_e^z = \dfrac{U_t^2}{2}\sin(2\delta - 2\phi)(\dfrac{1}{X_q'} - \dfrac{1}{X_d'}) + \\ \dfrac{U_t^2\sin(\delta - \phi)E_q'}{X_d'} - \dfrac{U_t^2\cos(\delta - \phi)E_d'}{X_q'} \end{cases} \quad (3)$$

where δ^z and ω^z are the PMU measurements of rotor angle and rotor speed [31], and P_e^z is the active power measurement.

The covariance of measurement noise R_{k+1} is

$$R_{k+1} = diag\left(\sigma_{\delta_z}^2, \sigma_{\omega_z}^2, \sigma_{P_{e_z}}^2\right) \quad (4)$$

where $\sigma_{\delta_z}^2$ and $\sigma_{\omega_z}^2$ are the measurement variance of rotor angle and speed, and $\sigma_{P_{e_z}}^2$ is the variance of active power.

$$P_{e_z}^2 = \left(\frac{\partial P_e}{\partial U}\right)^2 \sigma_U^2 + \left(\frac{\partial P_e}{\partial \phi}\right)^2 \sigma_\phi^2 \tag{5}$$

where $\sigma_u = 0.2\%$, $\sigma_\phi = 0.2°$.

For ease of description, (1) is transformed the following continuous-time state space model [1], [16]:

$$\begin{cases} \dot{x} = F_C(x, u) + v_C \\ z = H_C(x, u) + w_C \end{cases}$$
$$x = \left[\delta, \omega, E_d', E_q'\right]^T$$
$$z = \left[\delta^z, \omega^z, P_e^z\right]^T$$
$$u = \left[T_m, E_f, U_t, \phi\right]^T \tag{6}$$

where x is the state vector, u is the input vector, and z is the measurement vector; the subscript "C" denotes the continuous-time model; $F(\cdot)$ and $H(\cdot)$ are respectively the state transition and output functions; v_C and w_C are the process and output noise.

B. PROBLEM FORMULATION

With a sampling interval Δt, a real-time DSE can be described as the following filtering problem: given inputs such as $T_m(j\Delta t), E_f(j\Delta t), U_t(j\Delta t), \varphi(j\Delta t)$ for $j = 1, 2, \cdots, k$ we want to estimate the states of synchronous machines including $\delta(k\Delta t)$, $\Delta\omega(k\Delta t)$.

To perform state estimation via the discrete measurements, the continuous-time model in (6) is discretized into a discrete-time one as follows:

$$\begin{cases} x_{k+1} = F(x_k, u_k) + v_k \\ z_{k+1} = H(x_{k+1}, u_{k+1}) + w_{k+1} \end{cases} \tag{7}$$

where the subscript "k" is the moment at $k\Delta t$; v_k and w_{k+1} are the system process and measurement noises, and their covariance are denoted by Q_k and R_{k+1}. In this study, the process noise v_k is assumed to follow a Gaussian distribution, while the distribution of the measurement noise may not be Gaussian.

III. ROBUST CUBATURE KALMAN FILTER

A. CUBATURE KALMAN FILTER

The classical CKF was originally proposed in [32], which can be divided into two parts: time prediction and measurement update. In time prediction, CKF obtains a set of equally weighted state cubature points according to the spherical-radical rule. It can obtain predicted state variable and error variance matrix. In measurement update, the predicted state variable is updated by using measurements in order to improve estimation accuracy. The detailed process of the CKF is given as follows:

1) Time Prediction

Suppose that the estimation error covariance at time step k is $P_{k|k}$ and its square-rooting matrix is $S_{k|k}$.

$$P_{k|k} = S_{k|k} S_{k|k}^T \tag{8}$$

N cubature points of state variable are calculated.

$$X_{i,k|k} = S_{k|k} \zeta_i + \hat{x}_{k|k} \tag{9}$$

where $\hat{x}_{k|k}$ is the state estimatied valve at time step k. $X_{i,k|k}$ is the cubature point of $\hat{x}_{k|k}$, $\zeta_i = \sqrt{n}$, $i = 1, 2, \dots 2n$, n is the state vector dimension.

Through the state equations, the predicted values of the cubature points are obtained by

$$X_{i,k|k}^* = f\left(X_{i,k|k}, u_k\right) \tag{10}$$

where $X_{i,k+1|k}^*$ is the predicted value of $X_{i,k|k}$

The predicted values of state variable by weighted summation are obtained:

$$\hat{x}_{k+1|k} = \frac{1}{2n} \sum_{i=1}^{2n} X_{i,k+1|k}^* \tag{11}$$

where $\hat{x}_{k+1|k}$ is the predicted value of state variable.

The predicted error variance matrix of the state variable is

$$P_{k+1|k} = \frac{1}{2n} \sum_{i=1}^{2n} X_{i,k+1|k}^* X_{i,k+1|k}^{*T} - \hat{x}_{k+1|k} \hat{x}_{k+1|k}^T + Q_k \tag{12}$$

where $P_{k+1|k}$ is the predicted error variance matrix of state variable. Q_k is the covariance of process noise.

2) Measurement Update

The square-rooting matrix of predicted error covariance is calculated according to

$$P_{k+1|k} = S_{k+1|k} S_{k+1|k}^T \tag{13}$$

where $S_{k+1|k}$ is its square-rooting matrix.

N Cubature points of $\hat{x}_{k+1|k}$ are calculated by

$$X_{i,k+1|k} = S_{k+1|k} \zeta_i + \hat{x}_{k+1|k} \tag{14}$$

where $X_{i,k+1|k}$ is the cubature point of $\hat{x}_{k+1|k}$.

N Cubature points of predicted measurement are

$$Z_{i,k+1|k} = h\left(X_{i,k+1|k}, u_k\right) \tag{15}$$

where $Z_{i,k+1|k}$ is the cubature point of predicted measurement.

The predicted measurement by weighted summation are

$$\hat{z}_{k+1|k} = \frac{1}{2n} \sum_{i=1}^{2n} Z_{i,k+1|k} \tag{16}$$

where $\hat{z}_{k+1|k}$ is the predicted measurement.

The innovation covariance matrix of measurement error is given by

$$P_{zz,k+1|k} = \frac{1}{2n} \sum_{i=1}^{2n} Z_{i,k+1|k} Z_{i,k+1|k}^T$$
$$- \hat{z}_{k+1|k} \hat{z}_{k+1|k}^T + R_{k+1} \tag{17}$$

where $P_{zz,k+1|k}$ is the innovation covariance matrix. R_{k+1} is the covariance of measurement noise.

The cross-covariance matrix $P_{xz,k+1|k}$ is obtained by

$$P_{xz,k+1|k} = \frac{1}{2n} \sum_{i=1}^{2n} X_{i,k+1|k} Z_{i,k+1|k}^T - \hat{x}_{k+1|k} \hat{z}_{k+1|k}^T \quad (18)$$

where $P_{xz,k+1|k}$ is the cross-covariance matrix.

The filter gain W is obtained by

$$W_{k+1} = P_{xz,k+1|k} P_{zz,k+1|k}^{-1} \quad (19)$$

The estimated values of state variable are obtained by:

$$\hat{x}_{k+1|k+1} = \hat{x}_{k+1|k} + W_{k+1} \left(z_{k+1} - \hat{z}_{k+1|k} \right) \quad (20)$$

where W_{k+1} is the filter gain. $\hat{x}_{k+1|k+1}$ is the state estimated valve at time step $k + 1$.

The estimation error covariance $P_{k+1|k+1}$ is updated for the next time step:

$$P_{k+1|k+1} = P_{k+1|k} - W_{k+1} P_{zz,k+1|k} W_{k+1}^T \quad (21)$$

B. ROBUST CUBATURE KALMAN FILTER

As a nonlinear filtering technique, the conventional CKF needs an accurate system model and noise statistical characteristics to work well. However, the measurement noise may not obey the Gaussian assumption in the actual scene. More importantly, the noise statistical characteristics might change due to the influence resulted from internal or external unknown factors during the estimation process. When outliers occur in PMU measurements, the covariance matrix of measurement noises R will not consist with actual errors, and thereby the covariance matrix P_{zz} in (17) is unavailable to reflect the deviation of predicted value, which eventually leads to an inaccurate estimation. These above factors, to a certain extent, limits the usefulness and practicality of the CKF in actual applications.

The robust M-estimation theory is an effective tool for addressing robust estimation against unknown noise statistics [33]. Through robust M-estimation, we can detect the outliers on state estimation and update the statistical characteristics of the measurement noise in real time, which makes CKF capable of adapting to the statistical characteristics of measurement noises. By combining the Huber's M-estimation theory with the classical CKF, the proposed RCKF can obtain the accurate DSE of synchronous generators with unknown measurement noise statistics.

The RCKF uses the Huber's M-estimation approach to obtain a revised covariance matrix of measurement noises P_{zz} in (17). The corrected matrix $\bar{R}_{k+1}$ is substituted for the covariance of measurement noise in (17) as

$$\bar{R}_{k+1} = \bar{P}^{-1} \quad (22)$$

where the Huber's algorithm is utilized to calculate the equally weighted matrix $\bar{P}$.

Huber's M-estimation minimizes the cost function as

$$J(x_k) = \sum_{i=1}^{2n} \rho \left(r_i' \right) \quad (23)$$

where r_i' refers the ith component of the residual vector

$$r_i' = r_i / \sigma_{ri} \quad (24)$$

The r_i and its standard deviation σ_{ri} are calculated by

$$r_i = (z_{k+1} - \hat{z}_{k+1|k})_i \quad (25)$$
$$\sigma_{ri} = (P_{zz,k+1|k})_{i,i} \quad (26)$$

And the 'score function' $\rho(\cdot)$ is defined as

$$\rho(r_i') = \begin{cases} \frac{1}{2} r_i'^2, & \left| r_i' \right| \leq c \\ c \left| r_i' \right| - \frac{1}{2} c^2, & \left| r_i' \right| > c \end{cases} \quad (27)$$

where c is a constant and is chosen as 1.5 in this paper.

Setting the partial derivative of (23) to be zero gives

$$\sum_{i=1}^{2n} \frac{\partial \rho(r_i')}{\partial (r_i')} \cdot \frac{\partial (r_i')}{x_{k,i}} \quad i = 1, 2, ...n \quad (28)$$

where $x_{k,i}$ is the ith component of state vector. Denoting

$$w_i = \frac{\partial (r_i')}{r_i' \partial r_i'}, \quad i = 1, 2, ..2n \quad (29)$$

The formulation can be obtained

$$w_i = \begin{cases} 1, & \left| r_i' \right| \leq c \\ \frac{c}{\left| r_i' \right|}, & \left| r_i' \right| > c \end{cases} \quad (30)$$

Based on the above formulation, the equally weighted matrix $\bar{P}$ can be obtained as

$$\bar{p} \{i, i\} = \begin{cases} \frac{1}{\sigma_{i,i}}, & (\left| \frac{r_i}{\sigma_{ri}} \right| = \left| r_i' \right| \leq c) \\ \frac{c}{\sigma_{i,i} \left| r_{i,i} \right|}, & (\left| r_i' \right| > c) \end{cases} \quad (31)$$

$$\bar{p} \{i, j\} = \begin{cases} \frac{1}{\sigma_{i,j}}, & (\left| r_i' \right| \leq c, \left| r_i' \right| \leq c) \\ \frac{c}{\sigma_{i,j} \max(\left| r_i' \right|, \left| r_j' \right|)}, & (\left| r_i' \right| > c, \left| r_j' \right| > c) \end{cases} \quad (32)$$

where $\bar{p} \{i, i\}$ and $\bar{p} \{i, j\}$ are diagonal and off-diagonal elements of matrix $\bar{P}$; $\sigma_{i,i}$ and $\sigma_{i,j}$ are diagonal and off-diagonal elements in measurement noise matrix R_{k+1}. Since the measurement noise covariance matrix is a diagonal matrix, $\sigma_{i,j}$ is zero. r_i is the residual of measurement, r_i' is the standard residual error, σ_{ri} is the mean variance of r_i.

IV. CASE STUDIES

The proposed approach is tested on two systems, which are extracted from Power System Toolbox (PST) [34], and is compared with the original CKF in [25]. All the simulations are carried out on a PC with Intel Core i3-2330 2.20 GHz processor and 4 GB RAM.

The detailed simulation settings are listed as follow: 1) The simulation time step is set to 0.02 s; 2) The standard deviations of the rotor speed (p.u.) and rotor angle (°) are set to 0.001 p.u. and 2°; 3) The standard deviations of the amplitude and phase angle of the output voltage are taken as 0.1% and 0.1°; 4) Each generator is equipped with a PMU at its terminal; 5) PMU measurements are assumed to be sampled at 50 samples/s.

A. NOISE MODEL

We consider four types of noise: Gaussian white noise, Gaussian noise, Laplace noise, and Cauchy noise, which are respectively called noises 1-4.

1) GAUSSIAN WHITE NOISE AND GAUSSIAN NOISE

Gaussiannoiseisobtainedby

$$f(x) = \frac{1}{\sigma\sqrt{2\pi}} e^{-\frac{(l-\mu)^2}{2\sigma^2}} \tag{33}$$

where μ and σ are, respectively, the mean value and standard deviation of noise. When $\mu = 0$ and σ^2 is constant, we can obtain Gaussian white noise. If $\mu \neq 0$, we can obtain Gaussian noise.

2) LAPLACE NOISE

Laplace noise with scale s and mean μ is modeled as [3]

$$r_{Laplace} = \mu - s \times sgn(U_1)\ln(1 - |U_1|) \tag{34}$$

where s is the scale parameter (s is taken as $\sigma/\sqrt{2}$) and U_1 is a random parameter that obeys uniform distribution in the sampling interval.

3) CAUCHY NOISE

Cauchy noise is generated by [3]

$$r_{Cauchy} = a + b\tan(\pi(U_2 - 0.5)) \tag{35}$$

where a and b are the location and scale parameters, and U_2 is a random parameter that follows uniform distribution in the sampling interval. Here, a and b are respectively chosen as 10σ and σ. The parameters are given in Table 1.
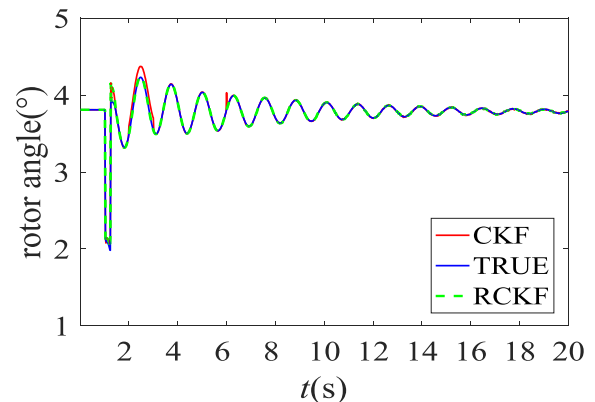
Two widely-used classical indicators proposed in [35] are here utilized to evaluate the performance of the estimation.

$$\varepsilon_1 = \sqrt{\frac{\sum\limits_{i=1}^{S_M} (\hat{x}_i - x_i^t)^2}{\sum\limits_{i=1}^{S_M} (x_i^z - x_i^t)^2}} \tag{36}$$

$$\varepsilon_2 = \sqrt{\frac{1}{S_M}\sum\limits_{i=1}^{S_M} \left(\frac{\hat{x}_i - x_i^t}{x_i^t}\right)^2} \tag{37}$$

TABLE 1. Noise types and parameters.

Noise type	Parameters	Standard deviation	Mean value
Noise 1	degree (°)	2	0
	ω (%)	0.1	0
Noise 2	degree (°)	2	20
	ω (%)	0.1	1
Noise 3	degree (°)	2	20
	ω (%)	0.1	1
Noise 4	degree (°)	2	20
	ω (%)	0.1	1

FIGURE 1. Rotor angle in Gaussian white noise.

where $\hat{x}_i$, x_i^t, x_i^z are the estimation value, true value, and the measurement value of the sampling point i, and S_M is the number of time steps.

B. CASE 1: WSCC 3-MACHINE 9-BUS SYSTEM

A three-phase short-circuit permanent fault is applied at bus 5 to generate dynamic responses at $t = 1.2$s. Then, the fault is cleared within the typical clearing time (5 cycles). The stimulation lasts for 20s. In real-world applications, bad PMU data must inevitably occur because of various causes such as impulsive noise, communication failures and potential/current transformer saturations, which leads to the severe deviation from the assumption that measurement noises obey the Gaussian distribution. To test the robustness of the proposed approach, two outlier scenarios are considered and tested, where a single outlier and a group of successive outliers are respectively added in the following two manners:

Manner 1: supposing that the rotor speed measurements are corrupted with 10% errors at the 6th second;

Manner 2: supposing that the rotor speed measurements are corrupted with 10% errors from $t = 2$s to $t = 3$s.

Taking generator 1 as an example, the estimation results under different types of noises are demonstrated in Figs. 1-8.

From Figs. 1-8, it can be seen that the filtering performance the RCKF is superior to that of the CKF in the following two aspects. 1) Concerning the same noise: the RCKF has good robustness in the presence of outliers; 2) Regarding various measurement noises, the RCKF shows good tracking and
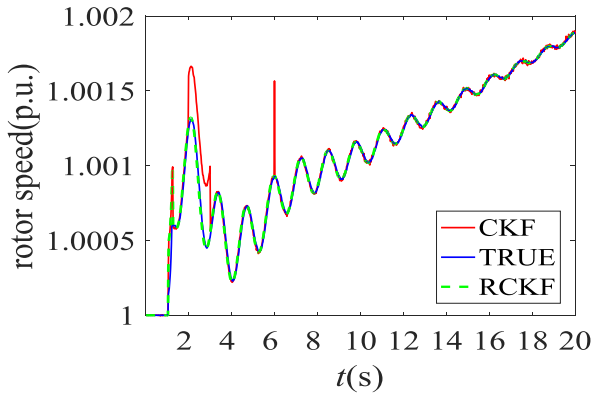
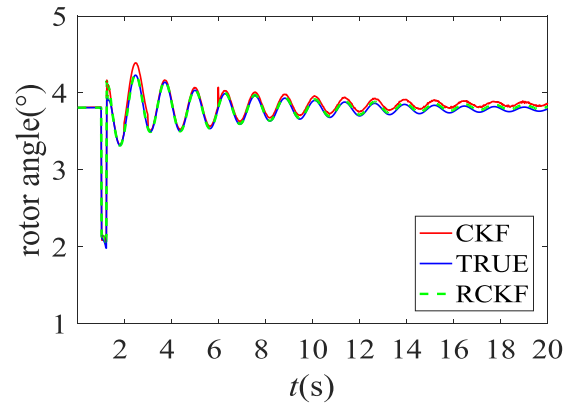**FIGURE 2.** Rotor speed in Gaussian white noise.
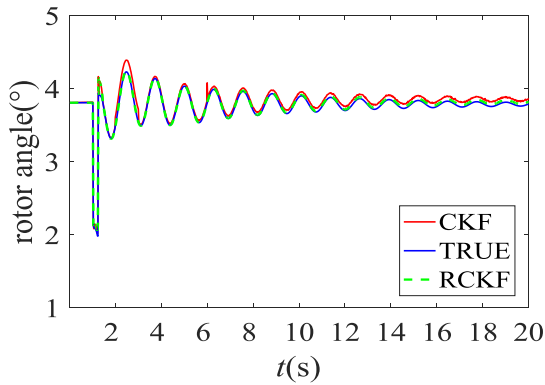

FIGURE 3. Rotor angle in Gaussian noise.

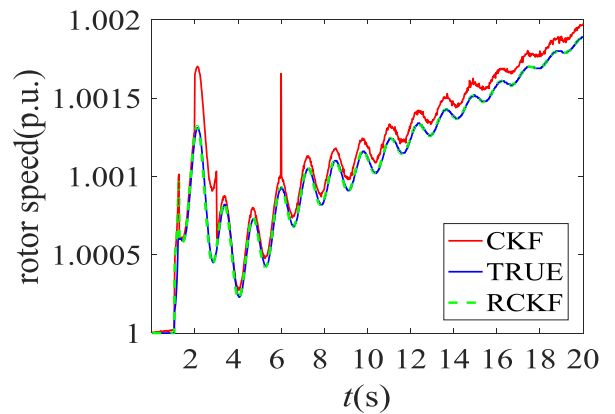**FIGURE 4.** Rotor speed in Gaussian noise.

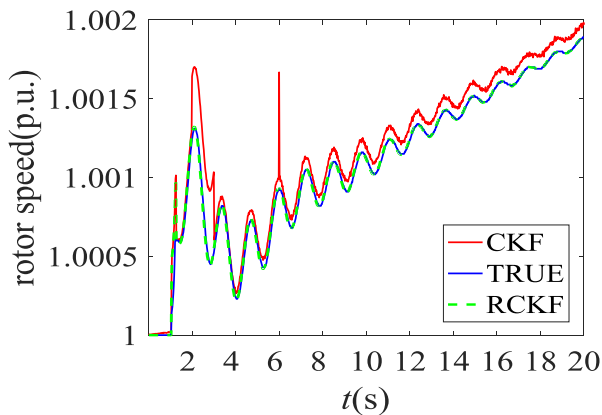**FIGURE 5.** Rotor angle in Laplace noise.
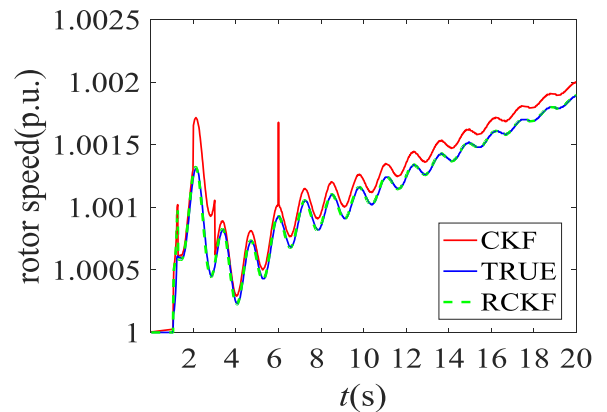

FIGURE 6. Rotor speed in Laplace noise.

FIGURE 7. Rotor angle in Cauchy noise.

convergence performance; while the performance of the CKF declines markedly. This is because the RCKF can detect outliers and update the statistical characteristics of the measurement noises via the Huber's M-estimation theory. By doing so, the estimated values of the RCKF can always converge to the true values accurately.

The quantitative comparison results of the two algorithms are demonstrated in Table 2.

From the above table, it can be observed that our approach outperforms the original CKF in the following two aspects.

(1) Regarding the indicator ε_1: in the case of noise 1, the indicator values of the RCKF are respectively increased by 52.7% and 60.9% compared with those of the CKF for rotor angle and rotor speed; in term of noise 2, they are increased by 65.6% and 69.5%; with noise 3, they are increased by 62.5% and 69.3%; with noise 4, they are increased by 51.7% and 64.4%. (2) In terms of the indicator ε_2: it can be seen that the filtering performance of the CKF significantly decreases in the case of non-Gaussian white noises (noises 2-4); while that
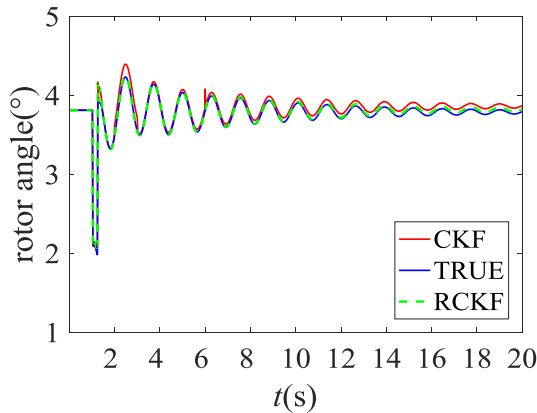
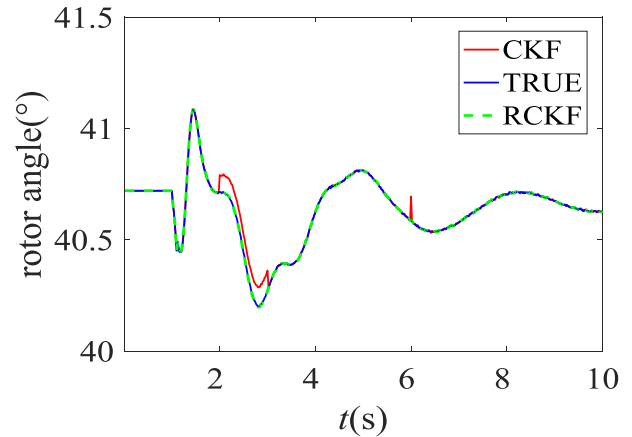**FIGURE 8.** Rotor speed in Cauchy noise.

TABLE 2. Dynamic state estimation indexes of generator 2.

Noise type	index	Variables	CKF	RCKF
Noise 1	ε_1	δ	0.0181	0.0085
		ω	0.0041	0.0016
	ε_2	δ	0.0248	0.0149
		ω	0.0011	4.574e-04
Noise 2	ε_1	δ	0.0032	0.0011
		ω	0.0046	0.0014
	ε_2	δ	0.0388	0.0164
		ω	0.0029	4.577e-04
Noise 3	ε_1	δ	0.0032	0.0012
		ω	0.0049	0.0015
	ε_2	δ	0.0387	0.0164
		ω	0.0031	4.579e-04
Noise 4	ε_1	δ	0.0029	0.0014
		ω	0.0045	0.0016
	ε_2	δ	0.0369	0.0170
		ω	0.0025	4.379e-04

of the RCKF has remained almost unchanged for all noises. This suggests that the RCKF can maintain good tracking performances under different noises.

It's worth noting that, as can be seen from (36), the indicator ε_1 of generator rotor angle δ in Noise 1 is significantly greater than those in other noises since the variance of measurement errors is much less than other types of noises, as shown in (36). Therefore, the RCKF has good adaptability to unknown measurement noise statistics, and it can detect and eliminate the outliers in the measurements.

C. CASE 2: NEW ENGLAND 16-MACHINE 68-BUS SYSTEM

This system includes 16 synchronous generators and 68 buses [3], [23]. A three-phase short-circuit fault is applied at bus 6 to generate a dynamic response at $t = 1$s. The fault will be cleared at near and remote ends after 0.05s and 0.1s. The simulation lasts for 10s. One single outlier is superimposed on the 6th second, and 10 continuous outliers are superimposed from the third second. As the same in Case 1, two outlier scenarios are considered and tested, where a single
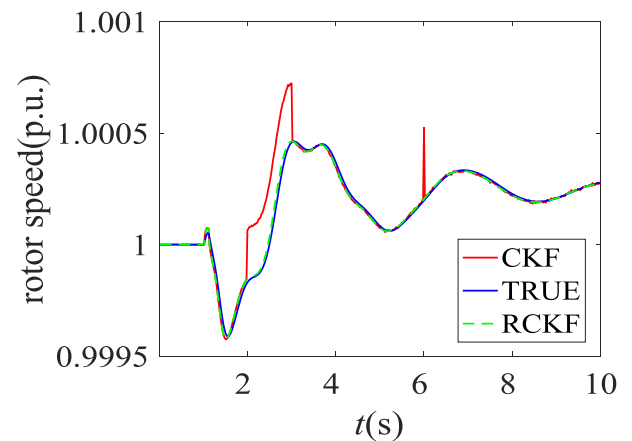

FIGURE 9. Rotor angle in Gaussian white noise.

FIGURE 10. Rotor speed in Gaussian white noise.

outlier and a group of successive outliers are respectively added in the following two manners:

Manner 1: supposing that the rotor speed measurements are corrupted with 10% errors at the 6th second;

Manner 2: supposing that the rotor speed measurements are corrupted with 10% errors from $t = 2$s to $t = 3$s.

Taking generator 1 as an instance, the dynamic state estimation results on the New England 68-bus system are demonstrated as Figs. 9-16 and Table 3.

From Figs. 9-16, it can be observed that: the RCKF has better filtering performance than that of the CKF under various noises. Especially, in the case of non-Gaussian noises, the performance of the CKF becomes clearly poor while the RCKF can still maintain good estimation accuracy and convergence.

From TABLE 3, it can be seen that: (1) Regarding indicator ε_1: the indicator value of the RCKF are respectively increased by 88.5% and 82.7% compared with those of the CKF for rotor angle and rotor speed under noise 1; they are increased by 89.4% and 84.9% under noise 2; they are increased by 90.0% and 73.7% under noise 3; they are increased by 88.7% and 83.8% under noise 4. (2) Concerning indicator ε_2: it can be observed that the performance of the CKF clearly
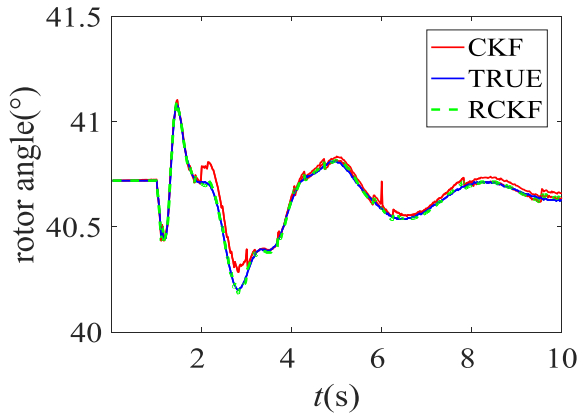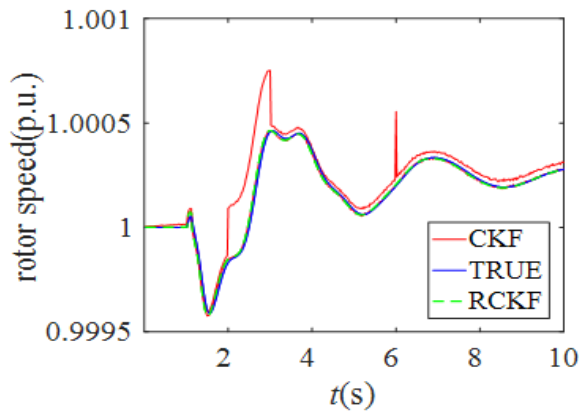
FIGURE 11. Rotor angle in Gaussian noise.

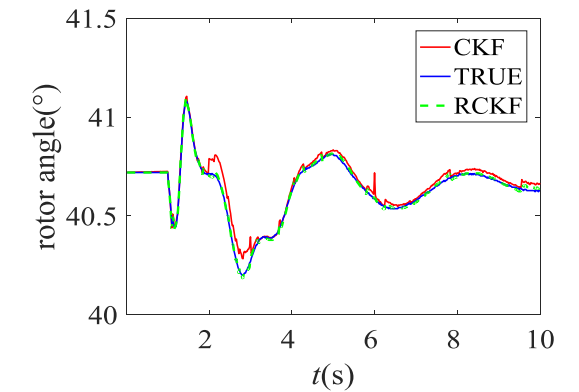**FIGURE 12.** Rotor speed in Gaussian noisel.

FIGURE 13. Rotor angle in Laplace noise.

FIGURE 14. Rotor speed in Laplace noise.

FIGURE 15. Rotor angle in Cauchy noise.

FIGURE 16. Rotor speed in Cauchy noise.

deteriorates under non-Gaussian white noises; while that of the RCKF has remained almost unchanged over all noises. Based on these results, a conclusion can be drawn that the proposed approach also manages to perform the DSE of synchronous machines for a larger power system.

D. COMPUTATIONAL EFFICIENCY
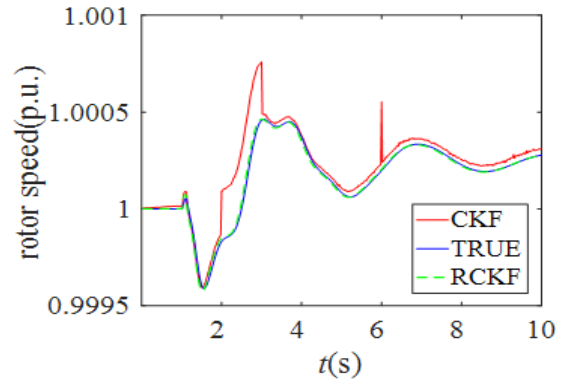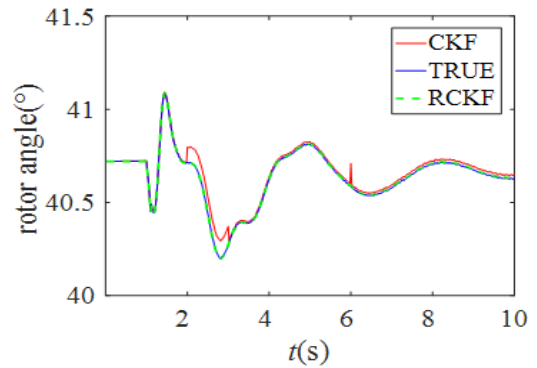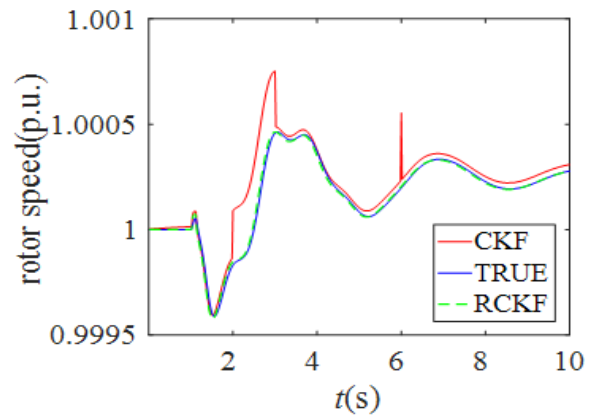In order to properly evaluate the computational efficiencies of the proposed RCKF, the computation time for a single generator by using the CKF and RCKF in the above two cases are demonstrated in Table 4.

The results in Table 4 show that the required computation times of the both algorithms are comparative, and the times are far less than a PMU sampling interval. This suggests that our approach is efficient enough to track the dynamic states of synchronous machines in real time, which is especially valuable for real-time applications such as emergency control. The computation time of the RCKF is only slightly more than that of the CKF. This is because additional computation

TABLE 3. Estimation results of generator 1 in 16 machines system.

Noises	index	Variables	CKF	RCKF
Noise 1	ε_1	δ	0.014	0.0016
		ω	0.0027	4.678e-4
	ε_2	δ	0.0044	7.176e-4
		ω	7.909e-4	2.124e-4
Noise 2	ε_1	δ	0.0017	1.800e-4
		ω	0.0027	4.06e-4
	ε_2	δ	0.0091	9.496e-4
		ω	0.0012	2.121e-4
Noise 3	ε_1	δ	0.0018	1.801e-4
		ω	0.0027	4.093e-4
	ε_2	δ	0.0096	9.501e-4
		ω	0.0012	2.3744-4
Noise 4	ε_1	δ	0.0020	2.257e-4
		ω	0.0028	4.232e-4
	ε_2	δ	0.0079	0.0064
		ω	0.0011	2.126e-4

TABLE 4. Calculating times of the CKF and RCKF.

Cases	Noises	CKF (ms)	RCKF (ms)
Case 1	Noise 1	0.301	0.362
	Noise 2	0.323	0.335
	Noise 3	0.325	0.341
	Noise 4	0.312	0.335
Case 2	Noise 1	0.237	0.252
	Noise 2	0.243	0.267
	Noise 3	0.195	0.217
	Noise 4	0.280	0.302

is needed for the robust M-estimation to detect outliers and gross error in measurements and for eliminating them by revising the measurement noise covariance matrix.

V. CONCLUSIONS

To resolve the lack of adaptability to unknown measurement noises using Kalman-type filtering techniques, a RCKF-based DSE approach for synchronous machines is proposed in this paper. By combing with the Huber's M-estimation theory and the original CKF, the proposed RCKF can detect outliers and gross errors, and thereby eliminate them by revising measurement noise variance matrix, which yields a more stable robust estimation. Finally, the simulation results of the WSCC 3-machine 9-bus system and New England 16-machine 68-bus system show that the presented approach has good robustness with outliers and good adaptability with unknown measure noises. More importantly, the filtering performances of the RCKF are far superior to those of the CKF against all types of noises used in this work.

Our future work will focus on extending this study to extensive potential applications in a whole power system. In addition, more realistic modeling techniques such as model uncertainties [36] and unknown inputs [37] will be incorporated to improve the practicality of our approach. Another interesting topic is to use the proposed algorithm for

solving other estimation problems in engineering, such as state of charge estimation of battery storage [38], [39] and state estimation in combined heat and power networks [40].

REFERENCES

[1] N. Zhou, D. Meng, and S. Lu, "Estimation of the dynamic states of synchronous machines using an extended particle filter," *IEEE Trans. Power Syst.*, vol. 28, no. 4, pp. 4152–4161, Nov. 2013.

[2] J. Zhao, M. Netto, and L. Mili, "A robust iterated extended Kalman filter for power system dynamic state estimation," *IEEE Trans. Power Syst.*, vol. 32, no. 4, pp. 3205–3216, Jul. 2017.

[3] J. Qi, A. F. Taha, and J. Wang, "Comparing Kalman filters and observers for power system dynamic state estimation with model uncertainty and malicious cyber attacks," *IEEE Access*, vol. 6, pp. 77155–77168, Dec. 2018.

[4] Y. Li et al., "Optimal scheduling of isolated microgrid with an electric vehicle battery swapping station in multi-stakeholder scenarios: A bi-level programming approach via real-time pricing," *Appl. Energy*, vol. 232, pp. 54–68, Dec. 2018.

[5] Y. Li, Z. Yang, G. Li, D. Zhao, and W. Tian, "Optimal scheduling of an isolated microgrid with battery storage considering load and renewable generation uncertainties," *IEEE Trans. Ind. Electron.*, vol. 66, no. 2, pp. 1565–1575, Feb. 2019.

[6] V. Terzija et al., "Wide-area monitoring, protection, and control of future electric power networks," *Proc. IEEE*, vol. 99, no. 1, pp. 80–93, Jan. 2011.

[7] A. S. Debs and R. E. Larson, "A dynamic estimator for tracking the state of a power system," *IEEE Trans. Power App. Syst.*, vol. PAS-89, no. 7, pp. 1670–1678, Sep. 1970.

[8] Z. Huang, K. Schneider, and J. Nieplocha, "Feasibility studies of applying Kalman filter techniques to power system dynamic state estimation," in *Proc. Int. Power Eng. Conf. (IPEC)*, Dec. 2007, pp. 376–382.

[9] E. Ghahremani and I. Kamwa, "Dynamic state estimation in power system by applying the extended Kalman filter with unknown inputs to phasor measurements," *IEEE Trans. Power Syst.*, vol. 26, no. 4, pp. 2556–2566, Nov. 2011.

[10] E. Ghahremani and I. Kamwa, "Online state estimation of a synchronous generator using unscented Kalman filter from phasor measurements units," *IEEE Trans. Energy Convers.*, vol. 26, no. 4, pp. 1099–1108, Dec. 2011.

[11] J. M. Park, C. K. Ahn, Y. S. Shmaliy, and M. T. Lim, "Improving reliability of particle filter-based localization in wireless sensor networks via hybrid particle/FIR filtering," *IEEE Trans. Ind. Informat.*, vol. 11, no. 5, pp. 1089–1098, Oct. 2015.

[12] K. Emami, T. Fernando, H. H. C. Iu, H. Trinh, and K. P. Wong, "Particle filter approach to dynamic state estimation of generators in power systems," *IEEE Trans. Power Syst.*, vol. 30, no. 5, pp. 2665–2675, Sep. 2015.

[13] L. Hu, Z. Wang, I. Rahman, and X. Liu, "A constrained optimization approach to dynamic state estimation for power systems including PMU and missing measurements," *IEEE Trans. Control Syst. Technol.*, vol. 24, no. 2, pp. 703–710, Mar. 2016.

[14] E. Ghahremani and I. Kamwa, "Local and wide-area PMU-based decentralized dynamic state estimation in multi-machine power systems," *IEEE Trans. Power Syst.*, vol. 31, no. 1, pp. 547–562, Jan. 2016.

[15] L. Fan and Y. Wehbe, "Extended Kalman filtering based real-time dynamic state and parameter estimation using PMU data," *Electr. Power Syst. Res.*, vol. 103, pp. 168–177, Oct. 2013.

[16] C. Wang, Z. Qin, Y. Hou, and J. Yan, "Multi-area dynamic state estimation with PMU measurements by an equality constrained extended Kalman filter," *IEEE Trans. Smart Grid*, vol. 9, no. 2, pp. 900–910, May 2018.

[17] A. Paul, I. Kamwa, and G. Jóos, "Centralized dynamic state estimation using a federation of extended Kalman filters with intermittent PMU data from generator terminals," *IEEE Trans. Power Syst.*, vol. 33, no. 6, pp. 6109–6119, Nov. 2018.

[18] A. Rouhani and A. Abur, "Constrained iterated unscented Kalman filter for dynamic state and parameter estimation," *IEEE Trans. Power Syst.*, vol. 33, no. 3, pp. 2404–2414, May 2018.

[19] J. Qi, K. Sun, J. Wang, and H. Liu, "Dynamic state estimation for multi-machine power system by unscented Kalman filter with enhanced numerical stability," *IEEE Trans. Smart Grid*, vol. 9, no. 2, pp. 1184–1196, Mar. 2018.

[20] A. K. Singh and B. C. Pal, "Decentralized dynamic state estimation in power systems using unscented transformation," *IEEE Trans. Power Syst.*, vol. 29, no. 2, pp. 794–804, Mar. 2014.

[21] N. Zhou, D. Meng, Z. Huang, and G. Welch, "Dynamic state estimation of a synchronous machine using PMU data: A comparative study," *IEEE Trans. Smart Grid*, vol. 6, no. 1, pp. 450–460, Jan. 2015.

[22] S. Wang, W. Gao, and A. P. S. Meliopoulos, "An alternative method for power system dynamic state estimation based on unscented transform," *IEEE Trans. Power Syst.*, vol. 27, no. 2, pp. 942–950, May 2012.

[23] G. Anagnostou and B. C. Pal, "Derivative-free Kalman filtering based approaches to dynamic state estimation for power systems with unknown inputs," *IEEE Trans. Power Syst.*, vol. 33, no. 1, pp. 116–130, Jan. 2018.

[24] A. Rouhani and A. Abur, "Linear phasor estimator assisted dynamic state estimation," *IEEE Trans. Smart Grid*, vol. 9, no. 1, pp. 211–219, Jan. 2018.

[25] L. Chen, T. S. Bi, and J. S. Li, "Dynamic state estimator for synchronous machines based on cubature Kalman filter," *Proc. CSEE*, vol. 34, no. 16, pp. 2706–2713, Jun. 2014.

[26] A. Sharma, S. C. Srivastava, and S. Chakrabarti, "A cubature Kalman filter based power system dynamic state estimator," *IEEE Trans. Instrum. Meas.*, vol. 66, no. 8, pp. 2036–2045, Aug. 2017.

[27] M. Rostami and S. Lotfifard, "Distributed dynamic state estimation of power systems," *IEEE Trans. Ind. Informat.*, vol. 14, no. 8, pp. 3395–3404, Aug. 2018.

[28] S. Wang, J. Zhao, Z. Huang, and R. Diao, "Assessing Gaussian assumption of PMU measurement error using field data," *IEEE Trans. Power Del.*, vol. 33, no. 6, pp. 3233–3236, Dec. 2018.

[29] B. Cui, X. Chen, X. Tang, H. Huang, and X. Liu, "Robust cubature Kalman filter for GNSS/INS with missing observations and colored measurement noise," *ISA Trans.*, vol. 72, pp. 138–146, Jan. 2018.

[30] J. Zhao and L. Mili, "Robust unscented Kalman filter for power system dynamic state estimation with unknown noise statistics," *IEEE Trans. Smart Grid*, vol. 10, no. 2, pp. 1215–1224, Mar. 2019. doi: 10.1109/TSG.2017.2761452.

[31] F. P. de Mello, "Measurement of synchronous machine rotor angle from analysis of zero sequence harmonic components of machine terminal voltage," *IEEE Trans. Power Del.*, vol. 9, no. 4, pp. 1770–1777, Oct. 1994.

[32] L. Arasaratnam and S. Haykin, "Cubature Kalman filters," *IEEE Trans. Autom. Control*, vol. 54, no. 6, pp. 1254–1269, Jun. 2009.

[33] Ž. M. Durović and B. C. Kovačević, "Robust estimation with unknown noise statistics," *IEEE Trans. Autom. Control*, vol. 44, no. 6, pp. 1292–1296, Jan. 1999.

[34] J. H. Chow and K. W. Cheung, "A toolbox for power system dynamics and control engineering education and research," *IEEE Trans. Power Syst.*, vol. 7, no. 4, pp. 1559–1564, Nov. 1992.

[35] K.-R. Shih and S.-J. Huang, "Application of a robust algorithm for dynamic state estimation of a power system," *IEEE Trans. Power Syst.*, vol. 17, no. 1, pp. 141–147, Feb. 2002.

[36] M. Zorzi, "Robust Kalman filtering under model perturbations," *IEEE Trans. Autom Control.*, vol. 62, no. 6, pp. 2902–2907, Jun. 2017.

[37] J. Lavenius and L. Vanfretti, "PMU-based estimation of synchronous machines' unknown inputs using a nonlinear extended recursive three-step smoother," *IEEE Access*, vol. 6, pp. 57123–57136, Oct. 2018.

[38] Y. Li, B. Feng, G. Li, J. Qi, D. Zhao, and Y. Mu, "Optimal distributed generation planning in active distribution networks considering integration of energy storage," *Appl. Energy*, vol. 210, pp. 1073–1081, Jan. 2018.

[39] S. Peng, C. Chen, H. Shi, and Z. Yao, "State of charge estimation of battery energy storage systems based on adaptive unscented Kalman filter with a noise statistics estimator," *IEEE Access*, vol. 5, pp. 13202–13212, Jul. 2017.

[40] Y. Li, J. Wang, D. Zhao, G. Li, and C. Chen, "A two-stage approach for combined heat and power economic emission dispatch: Combining multi-objective optimization with integrated decision making," *Energy*, vol. 162, pp. 237–254, Nov. 2018.

Authors' photographs and biographies not available at the time of publication.

• • •